Membrane composition-mediated protein-protein interactions

Benedict J. Reynwar
Max-Planck-Institute for Polymer Research, Ackermannweg 10, 55128 Mainz, Germany

Markus Deserno[a)]
Department of Physics, Carnegie Mellon University, Pittsburgh, Pennsylvania 15213

(Received 12 March 2008; accepted 11 August 2008; published 7 January 2009)

The authors investigate membrane composition-mediated interactions between proteins adsorbed onto a two-component lipid bilayer close to critical demixing using coarse-grained molecular dynamics simulations and a phenomenological Ginzburg-Landau theory. The simulations consist of three-bead lipids and platelike proteins, which adsorb onto the membrane by binding preferentially to one of the two lipid species. The composition profile around one protein and the pair correlation function between two proteins are measured and compared to the analytical predictions. The theoretical framework is applicable to any scalar field embedded in the membrane, and although in this work the authors treat flat membranes, the methodology extends readily to curved geometries. Neglecting fluctuations, both lipid composition profile and induced protein pair potential are predicted to follow a zeroth order modified Bessel function of the second kind with the same characteristic decay length. These predictions are consistent with our molecular dynamics simulations, except that the interaction range is found to be larger than the single profile correlation length. [DOI: 10.1116/1.2977492]

I. INTRODUCTION

Biological membranes are two-dimensional fluid bilayers composed of a complex mixture of lipids and proteins. Traditionally they have been viewed as passive homogeneous structures whose task is to compartmentalize the cell and carry solubilized proteins.[1] This picture is now being replaced by that of a heterogeneously structured material actively participating in many cellular functions.[2–6] While *in vitro* experiments on ternary lipid mixtures have uncovered much about the physics of coexisting fluid lipid phases,[7–11] the precise connection between such simple model mixtures and biomembranes is still poorly understood,[12] even though macroscopic separation can be triggered in biological systems.[13] Besides thermodynamic phase separation, other mechanisms behind plasma membrane inhomogeneities have been proposed as well, such as nonequilibrium lipid or cholesterol transport processes,[14,15] and membrane interactions with the cytoskeleton.[16] In this article we study a particular kind of *equilibrium* inhomogeneity, namely, how the selective coupling of proteins to lipids in a near-critical but *not yet* segregated mixture can induce protein clustering.

The general idea that membrane-based fields can mediate interactions between membrane-associated proteins (provided they couple to it) is a very fruitful one and has been the subject of much research. In 1984 Mouritsen and Bloom[17] introduced the mattress model, which describes the interactions between hydrophobically mismatched proteins in a membrane and the resulting phase behavior. The treatment of the local elastic deformations was later refined by several other groups.[18–22] Coupling to a composition field was investigated in the context of wetting[23–26] and charge demixing.[27–29] Interactions mediated by curvature were first treated by Goulian *et al.*[30,31] and further discussed by many others.[32–46]

Besides a ground-state contribution each field can also mediate forces due to its *fluctuations*. This effect is now named after Casimir,[47] who used it to predict an attraction between conducting plates mediated by (quantum) fluctuations in the electromagnetic field. Later Fisher and de Gennes[48] discussed this phenomenon for classical critical fluctuations in a soft-matter context. Casimir forces were subsequently studied by many others, as summarized, for instance, by Krech.[49–51] Recently Hertlein *et al.*[52] measured them very accurately in a sphere-plate geometry and compared quantitatively to field-theoretical predictions. For lipid membranes Casimir forces were discussed in the context of near-critical scalar[53] or tensorial[54] order parameters, and for curvature fluctuations.[30–32,55–58]

The situation we investigate here is that of a binary lipid A-B mixture close to demixing. If proteins preferentially bind to one lipid species, say A, they will be surrounded by an A-rich halo that decays on a length scale that emerges from a balance between the penalty for (i) deviation from the preferred composition and (ii) creation of composition gradients. When two such proteins approach close enough for halo overlap to occur, a force is experienced, the sign of which depends on the lipid preference.

In this work we show that the effect of composition-driven protein interactions can be readily identified in suitably coarse-grained off-lattice membrane simulations. While the underlying physics is indeed well understood, it must be noted that actually *probing* it in a particle-based model is not trivial at all. Equilibrating lipid mixtures—particularly close to a critical point—is very difficult and was previously impossible with standard and even most coarse-grained simula-

a)Electronic mail: deserno@andrew.cmu.edu.

tion strategies. A lipid with a diffusion constant of $D \simeq 1\ \mu m^2/s$ takes about half a millisecond to diffuse over just 50 nm, a process which is therefore completely inaccessible in atomistic simulations. Since compositional fluctuations cannot only couple to proteins but also to the overall bilayer curvature, the possibility to access them in a large-scale particle-based membrane model therefore renders many exciting scientific questions accessible to simulation studies. However, before these can be explored, the scenario needs to be checked in simple cases for which (most of) the physics is essentially understood.

In order to rationalize our simulations, we use a simple ground-state treatment of an appropriate scalar ϕ^4 Ginzburg-Landau theory. Forces are obtained very efficiently as integrals over the associated stress tensor, an approach that remains valid for arbitrarily curved surfaces (i.e., in the nonlinear regime). Even without solving the field equations it shows in a transparent way that the sign of the composition-dependent component of the force follows from symmetry considerations. Being a ground-state treatment, our current analysis is not yet self-consistent at the critical temperature, but we suggest that it constitutes a useful and generalizable starting point for a covariant treatment of fluctuating geometries.

II. INTERACTIONS BETWEEN MEMBRANE-BOUND OBJECTS MEDIATED BY A SCALAR FIELD

Let us begin by summarizing the theoretical framework of a scalar field theory for mixed membranes. The approach is of course standard and has been used many times before in the literature, for instance, to study coupling between composition and shape,[59–61] and it has been linked to molecular dynamics (MD) simulations.[62–64] We will, however, present a very economical way to extract field-mediated interactions using a differential geometric language and subsequently compare the predictions with our coarse-grained simulations. In its current form our approach neglects fluctuation corrections that give rise to additional Casimir forces,[30–32,48–58,65,66] but the formalism can be extended toward fluctuating stresses.[50,67–69]

A. Energy functional

Consider a fluid membrane composed of a mixture of two different lipid species. Using the composition difference ϕ as the order parameter, this situation can be described by a simple membrane-associated Ginzburg-Landau theory[70–72] of the form

$$E[\phi] = \int \mathrm{d}A \left\{ \frac{1}{2} a (\nabla\phi)^2 + V(\phi) \right\}. \tag{1}$$

The integral extends over the (possibly curved) membrane area and $(\nabla\phi)^2$ is a short hand for the covariant squared gradient $(\nabla_a\phi)(\nabla^a\phi)$. As usual, the (ground-state) field equation follows from setting the functional derivative with respect to ϕ to zero:

$$0 = \frac{\delta E[\phi]}{\delta\phi} = -a\Delta\phi + \frac{\partial V}{\partial\phi}, \tag{2}$$

where $\Delta = \nabla_a\nabla^a$ is the Laplace-Beltrami operator. If the potential $V(\phi)$ has a minimum at $\phi = \phi_{\min}$, this (constant) field evidently solves the field equation.

Let there now be objects bound to (or inserted into) the membrane which couple to ϕ by imposing boundary conditions to it. The ground-state field will then be a solution of the field Eq. (2) subject to these boundary conditions, and the associated energy is the functional evaluated with this field: $E_{\mathrm{equi}} = E[\phi_{\mathrm{equi}}]$. With more than one object being present, the field—and thus its energy—will depend on their relative positions. This implies that field-mediated forces will generally act between the objects.

B. Forces via the stress tensor

Generalizing the well known formalism from classical elasticity theory,[73] forces on a membrane patch $\mathcal{P}$ can be obtained by a closed-loop integral over the flux of stress over the boundary of $\mathcal{P}$:

$$\boldsymbol{F} = -\oint_{\partial\mathcal{P}} \mathrm{d}s\, l_a \boldsymbol{f}^a, \tag{3}$$

where $l_a = \boldsymbol{l}\cdot\mathbf{e}_a$ are the coordinates of the outward pointing unit normal to $\partial\mathcal{P}$ that is tangential to the surface, and $\boldsymbol{f}^a$ is the surface stress tensor.[74–76] If particles are attached to the membrane and kept at some fixed distance, they act as external sources of stress. For each particle this force is picked up by such a closed-loop integral, provided it encircles this (and only this) particle.

For the energy functional (1) and in the context of membranes it has previously been shown that[75]

$$\boldsymbol{f}^a = \left[a(\nabla^a\phi)(\nabla^b\phi) - \left(\frac{a}{2}(\nabla\phi)^2 + V(\phi) \right) g^{ab} \right] \boldsymbol{e}_b, \tag{4}$$

where $g^{ab} = \boldsymbol{e}^a\cdot\boldsymbol{e}^b$ is the (inverse) metric tensor and $\boldsymbol{e}_a = \partial\boldsymbol{X}/\partial\xi^a$ are the tangent vectors, obtained by differentiating the surface embedding function $\boldsymbol{X}(\xi^1,\xi^2)$ with respect to the coordinates ξ^a. More background on the differential geometry can be found in Refs. 77 and 78.

We note that the stress tensor (4) of a Ginzburg-Landau ϕ^4 theory has also been used to calculate forces within the framework of statistical field theory.[49–51,67,68] In this case it is frequently amended by a so-called improvement term, which renders it traceless inside correlation functions at the Gaussian and Wilson-Fisher fixed points.[50,67,68] We will not include this term here.

C. Two-particle situation

We now look at the situation of two identical particles, both imposing a disturbance in the field. As indicated in Fig. 1, we can adapt the contour integral such that one branch passes exactly between the two particles. If ϕ vanishes at large distances from both particles, and if $V(0)=0$, the only contribution to the force integral (3) stems from this midline.

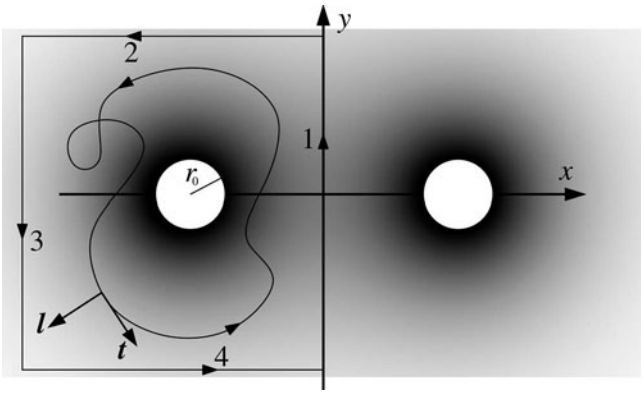

FIG. 1. Density field around two proteins. The force on the left one can be obtained as a contour integral of the flux of stress through any loop enclosing that particle [see Eq. (3)]. It is suitable, though, to choose the contour with some regard to symmetry, such as the sequence $1\to2\to3\to4$.

From completeness we get $l_a(\nabla^a\phi)(\nabla^b\phi)\boldsymbol{e}_b = (\nabla_\perp\phi)^2\boldsymbol{l}+(\nabla_\perp\phi)(\nabla_\parallel\phi)\boldsymbol{t}$. Here, $\boldsymbol{l}=l^a\boldsymbol{e}_a$ is again the outward pointing unit normal and $\boldsymbol{t}=t^a\boldsymbol{e}_a$ is the unit tangent vector to the contour. Furthermore, $\nabla_\perp=l^a\nabla_a$ and $\nabla_\parallel=t^a\nabla_a$ are the directional derivatives perpendicular and parallel to the contour. Since finally $(\nabla\phi)^2=(\nabla_\perp\phi)^2+(\nabla_\parallel\phi)^2$, we obtain the following remarkably simple expression for the force:

$$\boldsymbol{F}=-\int_1 ds\left\{\frac{a}{2}[(\nabla_\perp\phi)^2-(\nabla_\parallel\phi)^2]-V(\phi)\right\}\boldsymbol{l}. \tag{5}$$

This is an exact ground-state result. Notice that we have already eliminated the contribution proportional to $\boldsymbol{t}$, since the system also possesses mirror symmetry in the $x-z$ plane (see Fig. 1): on the midline $\phi(s)$, $\nabla_\perp\phi(s)$, and $\boldsymbol{t}(s)$ are even functions, while $\nabla_\parallel\phi(s)$ is odd, such that the integral over $(\nabla_\perp\phi)(\nabla_\parallel\phi)\boldsymbol{t}$ vanishes.

Let us specialize Eq. (5) to the two cases of *symmetry* and *antisymmetry* with respect to the y-axis in Fig. 1—i.e., to the two cases where the two proteins either induce the same field deviation from zero or opposite field deviations. In the symmetric case $\nabla_\perp\phi$ vanishes on the midline, while in the antisymmetric case both $\nabla_\parallel\phi$ and $V(\phi)$ vanish there. Hence, we get the two simplified formulas for the force acting on the left particle:

$$\boldsymbol{F}_{\text{sym}}=\int_1 ds\left\{\frac{a}{2}(\nabla_\parallel\phi)^2+V(\phi)\right\}\boldsymbol{l}, \tag{6a}$$

$$\boldsymbol{F}_{\text{antisym}}=-\int_1 ds\,\frac{a}{2}(\nabla_\perp\phi)^2\boldsymbol{l}. \tag{6b}$$

Notice that *without solving the field equations* we can already make nontrivial statements about the direction of the force induced by the composition field: In the symmetric case particles will attract, provided $V(\phi)\geq0$, while in the antisymmetric case particles will repel, provided that the membrane will not deform so much that $\boldsymbol{l}\cdot\boldsymbol{x}$ becomes negative.

D. Special case of a planar membrane

Let us assume that the potential $V(\phi)$ has a series expansion $V(\phi)=\frac{1}{2}t\phi^2+\frac{1}{4}u\phi^4+\cdots$. If we remain in the non-phase-segregated case, $t>0$ and we can restrict to the quadratic order. We now have the situation of a scalar field for which $\phi\equiv0$ is the (homogeneous) ground state. The field Eq. (2) then reduces to the differential equation $(\lambda^2\Delta-1)\phi=0$, where we introduced the characteristic length

$$\lambda:=\sqrt{a/t}. \tag{7}$$

If the membrane is planar, Δ simplifies to the ordinary Laplacian, and we arrive at a *linear* partial differential equation, the Helmholtz equation.

Let us solve this equation for one circular particle. Then, $\Delta=\partial_r^2+(1/r)\partial_r$ in polar coordinates. Defining $\tilde{r}=r/\lambda$, this equation reads $(\tilde{r}^2\partial_{\tilde{r}}^2+\tilde{r}\partial_{\tilde{r}}-\tilde{r}^2)\phi=0$. The solutions of this equation are the modified Bessel functions of first and second kind, $\mathrm{K}_0(\tilde{r})$ and $I_0(\tilde{r})$.[79] If the particle has a radius r_0 and imposes the field value $\phi(r_0)=\phi_0$ there, the final solution (regular at infinity) reads

$$\phi(\tilde{r})=\phi_0^*\mathrm{K}_0(\tilde{r}), \tag{8}$$

where we also defined the scaled radius $\tilde{r}_0=r_0/\lambda$ and the scaled amplitude $\phi_0^*=\phi_0/K_0(\tilde{r}_0)$.

The same equation cannot be solved nearly as simply if we have two particles at some distance d. We will instead employ the *Nicholson approximation* and assume that the field of the two-body problem is given by the superposition of the fields of two one-body problems.[80] The entire field of the two-particle problem is then

$$\begin{aligned}\phi_\pm(x,y)&=\phi_{\text{left}}(x,y)\pm\phi_{\text{right}}(x,y)\\&=\phi_0^*\left[K_0\left(\frac{\sqrt{y^2+(d/2+x)^2}}{\lambda}\right)\right.\\&\quad\left.\pm\ K_0\left(\frac{\sqrt{y^2+(d/2-x)^2}}{\lambda}\right)\right],\end{aligned} \tag{9}$$

where the "+" holds for the symmetric and the "–" for the antisymmetric case. Hence, the (x component of the) force is easily seen to be

$$F_+=\frac{2t\lambda\phi_0^2}{K_0^2(\tilde{r}_0)}\int_{-\infty}^{+\infty}d\eta\left\{\frac{\eta^2K_1^2(\sqrt{\eta^2+d^{\star2}})}{\eta^2+d^{\star2}}+K_0^2(\sqrt{\eta^2+d^{\star2}})\right\}, \tag{10a}$$

$$F_-=-\frac{2t\lambda\phi_0^2}{K_0^2(\tilde{r}_0)}\int_{-\infty}^{+\infty}d\eta\frac{\left(\frac{d^\star}{2}\right)^2K_1^2(\sqrt{\eta^2+d^{\star2}})}{\eta^2+d^{\star2}}. \tag{10b}$$

where $d^\star=d/2\lambda$. The solution to these force integrals, and the corresponding pair potentials, are given by

$$F_\pm(d)=\pm2\pi t\lambda\phi_0^{*2}K_1(d/\lambda), \tag{11a}$$

$$U_\pm(d)=\mp2\pi a\phi_0^{*2}K_0(d/\lambda). \tag{11b}$$

Symmetric and antisymmetric cases thus only differ by the *sign* of the interaction. Notice also the striking similarities

TABLE I. Table of all interaction potentials used in the simulations. The value of the bead diameter b for $U_{LJ}(r)$ and $U_{WCA}(r)$ depends on the type of beads involved: A lipid head bead meeting any other bead always has $b=0.95\sigma$, while lipid tail beads meet with $b=1\sigma$. The value of the potential range in $U_{\cos}(r)$ for homotypic interactions is always $w_c=1.6\sigma$, while for heterotypic interactions it is varied between $w_c=1.48\sigma$ and $w_c=1.6\sigma$. The temperature was always chosen as $k_BT=1.1\epsilon$.

Physically interacting units	Potential	Functional form	Range	Parameters
Adhesion between protein and membrane beads	$U_{LJ}(r)$	$4\alpha\epsilon\left[\left(\frac{b}{r}\right)^{12}-\left(\frac{b}{r}\right)^{6}\right]$	$0<r<r_{cut}$	$r_{cut}=2.5b$ $\alpha=2$
Hard core repulsion between all beads	$U_{WCA}(r)$	$4\epsilon\left[\left(\frac{b}{r}\right)^{12}-\left(\frac{b}{r}\right)^{6}+\frac{1}{4}\right]$	$0<r<r_{cut}$	$r_{cut}=2^{1/6}b$
Link between lipid beads	$U_{FENE}(r)$	$-\frac{1}{2}k_{FENE}r_\infty^2\ln\left(1-\frac{r^2}{r_\infty^2}\right)$	$0<r<r_\infty$	$k_{FENE}=30\epsilon/\sigma^2$ $r_\infty=1.5\sigma$
Effective bending potential to keep lipids roughly straight	$V_{bend}(r)$	$\frac{1}{2}k_{bend}(r-4\sigma)^2$	$0<r<\infty$	$k_{bend}=10\epsilon/\sigma^2$
Cohesion between lipid tail beads	$U_{\cos}(r)$	$-\varepsilon$ $-\epsilon\cos^2\frac{\pi(r-r_{cut})}{2w_c}$	$0<r<r_{cut}$ $r_{cut}\le r\le r_{cut}+w_c$	$r_{cut}=2^{1/6}\sigma$

(and differences!) to the case of a *vector* field discussed in Ref. 45. There the magnitude of the vector field decays like $K_1(r/\lambda)$ around a field exciting protein as a function of distance, yet the pair potential has again K_0 form. However, for vector fields the symmetric situation gives rise to a *repulsion*.

Even though the contact binding energy $U_{\pm}(2r_0)$ vanishes like $\pm 1/\ln(\lambda/r_0)$ for $\lambda\to\infty$, the *second virial coefficient* diverges asymptotically like $\pm\lambda^2/\ln^2(\lambda/r_0)$ in the same limit. The composition-mediated ground-state protein-protein interaction will therefore become very strong for $t\to 0$. Notice, however, that $t=0$ is the critical point of this theory, hence fluctuations will renormalize this ground-state result, in fact, significantly so in two dimensions.[72] Our theoretical analysis, while providing a simple explanation for the emergence of interactions, can therefore not be expected to be quantitatively correct.

III. SIMULATION METHOD

We used the ESPRESSO package[81] to perform MD simulations of coarse-grained lipid membranes. For the questions we are interested in, a very simple membrane model suffices, and we adopt the model developed by Cooke *et al.*[82] It owes its efficiency to (i) a rather minimal representation of lipids and (ii) its elimination of an explicit embedding solvent. More details on recent advances in coarse-grained lipid membrane simulations can be found in Refs. 83 and 84, and 85 specifically reviews solvent free approaches.

In the Cooke model a lipid molecule consists of a linear string of three beads: a head bead and two tail beads. The head beads interact with other head beads and with the tail beads through a short-range repulsive Weeks-Chandler-Anderson potential, $U_{WCA}(r)$, whereas the tail-tail interaction, $U_{\cos}(r)$, is longer-ranged and attractive. These potentials are given in Table I and were chosen such that the lipid molecules assemble into a stable bilayer. The w_c parameter in $U_{\cos}(r)$ controls the range of the attractive part of the potential. Cooke *et al.*[82] investigated the effect of this parameter on the lipid bilayer phase behavior: When it is large, the membrane become rigid (gel phase); when it is small, no self-assembly is possible. Intermediate values lead to the fluid phase which we study in this article.

The simulations we discuss here involve two lipid species, for simplicity termed types A and B. The lengths w_{AA}, w_{BB}, and w_{AB} refer to the values of the parameter w_c for the interaction range between two A lipids, two B lipids, and between an A and a B lipid, respectively. We chose $w_{AA}=w_{BB}=1.6\sigma$, implying that a pure A and a pure B phase have identical properties. The cross term w_{AB} is varied between 1.48σ and 1.6σ. In the latter case the membrane is really a one-component system. However, for $w_{AB}<1.6\sigma$ every AB contact lowers the membrane cohesion energy less than an AA or a BB contact. This results in a lipid incompatibility, nonideal mixing, and—for sufficiently small w_{AB}—a lipid phase segregation into an A-rich and a B-rich phase.

Our simulated model proteins consist of disks of two hexagonally packed layers of 19 beads, one on top of the other. The beads in the bottom layer interact favorably through a Lennard-Jones potential $U_{LJ}(r)$ with the head beads of lipids of type A. In contrast, lipids of type B interact with the proteins through a short-range repulsive WCA potential. The attractive interaction causes the proteins to adsorb *onto* the bilayer, creating an island enriched in A lipids underneath them. Notice that our proteins do not insert, hence no hydrophobic mismatch related interactions[17–22] are expected. The simulations are performed at a temperature of $k_BT=1.1\epsilon$ and a vanishing lateral tension, which is achieved by using a modified Andersen barostat.[86]

IV. SIMULATION RESULTS

A. Critical point and line tension

The critical point of the binary lipid mixture was determined by measuring the effect of w_{AB} on the line tension γ between the immiscible lipid phases in the segregated regime (i.e., for sufficiently small w_{AB}). We perform simulations of a patch of membrane of mean box size $80\sigma\times 80\sigma$. Initially the left half of the membrane patch was pure lipid A, whereas the right half was pure lipid B. Once the simulation was started we monitored the equilibration of the system by tracking the energy between A and B head beads, which increases at early times as the interfacial width broadens and more A-B contacts occur. For completely diffusive behavior one expects a concentration modulation of wavelength λ

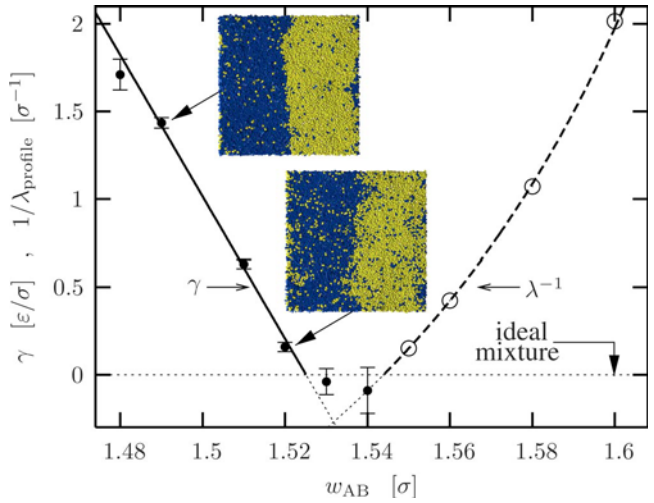

FIG. 2. (Color online) Line tension γ between A-rich and B-rich lipid phases (solid dots) and (inverse) correlation length λ in an A-B-mixture. The correlation length is determined from the decay length around a protein (see also Fig. 5 below). The two insets are equilibrated top-view snapshots from the simulation illustrating the morphology of the two lipid phase boundary close to and away from the critical point.

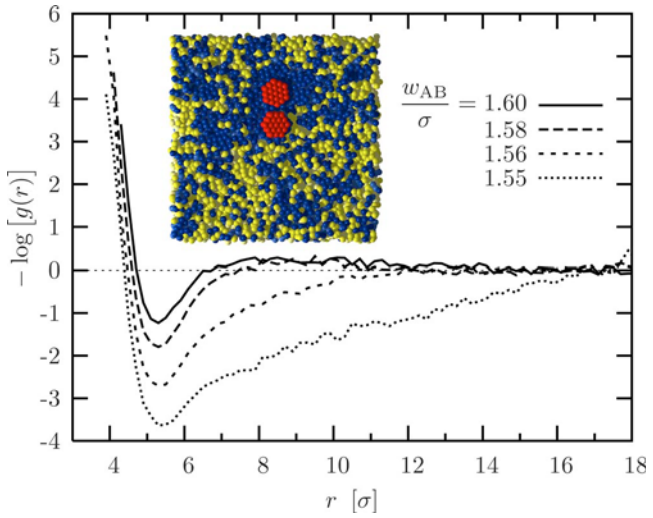

FIG. 3. (Color online) Pair potential between proteins as a function of separation r, $U_{\rm pair}(r)/k_BT=-\log[g(r)]$, obtained as the logarithm of the pair correlation function. The snapshot in the inset used $w_{\rm AB}=1.56\sigma$.

$=2\pi/k$ to decay at large times exponentially with a rate of $r_{\rm diff}=Dk^2$, where D is the lipid diffusion constant. For our system we have $D\simeq 0.01\sigma^2/\tau$ (Ref. 87) and $\lambda=L=80\sigma$, which gives a relaxation time of $r_{\rm diff}^{-1}\simeq 16000\tau$. For a completely compatible A-B mixture ($w_{\rm AB}=1.6\sigma$) this is indeed borne out by the simulation, showing that it takes almost $10^5\tau$ until the system is fully equilibrated. This is also the limiting time scale close to the critical point, since at low surface tension there is a significant fraction of A lipids in the B phase (and vice versa) which have to get there by diffusion (see the insets in Fig. 2). Getting equilibrated configurations of the phase boundary and thus values of the line tension therefore takes significant simulation time.

The line tension γ between the phases is measured by calculating the pressure tensor of the system. The presence of the interface means that the components of the pressure in the x and y directions differ on average. Since the total pressure is set to 0, the average pressure in the x direction is the negative of the average pressure in the y direction. The line tension is then the difference between the xx and yy components of the pressure tensor multiplied by the area over which the pressures acts (L_yL_z if the lines are in the x direction) and divided by two (there are two lines present in the system due to the periodic boundary conditions). Figure 2 shows the line tension as a function of $w_{\rm AB}$ in the regime where the system is phase separated (solid dots). From this the critical point appears to be bracketed between $w_{\rm AB}=1.52\sigma$ and 1.53σ.

B. Protein pairs

Having localized the critical point of our coarse-grained model, we investigate the behavior of proteins bound to a membrane with varying values of $w_{\rm AB}$ that are *larger* than the critical value (i.e., the mixed state). The inset of Fig. 3 shows a snapshot from a simulation with $w_{\rm AB}=1.56\sigma$. The centers of mass of the proteins were constrained to lie on a plane perpendicular to the membrane, so the pair correlation function $g(r)$ is simply the fraction of simulation snapshots in which the proteins were a distance r apart, normalized such that $g(r)\to 1$ at large separation. Since there are only two proteins in the simulation, the negative logarithm of $g(r)$ equals the pair potential in units of the thermal energy: $U_{\rm pair}(r)=-k_BT\ln[g(r)]$.

In Fig. 3 we plot this pair potential for four different levels of membrane immiscibility. An overall simulation time of 200 000τ is used. Even for *entirely compatible* lipids, which interact with one another as they interact with themselves ($w_{\rm AB}=w_{\rm AA}=w_{\rm BB}$), an attractive short-range interaction between the proteins remains, visible as a small minimum of order k_BT in the pair potential. We have not yet traced the origin of this noncompositional interaction, but various possibilities arise here, such as a depletion attraction induced by the close lipids, local packing effects, or a Casimir interaction due to fluctuations of the overall membrane shape ("undulations") or individual lipid positions ("protrusions"). When $w_{\rm AB}$ is decreased from 1.60σ to 1.58σ, the attractive interaction between the proteins is observed to grow stronger. For $w_{\rm AB}=1.56\sigma$, the minimum in $U_{\rm pair}(r)$ reaches $-2.7k_BT$ and a clear tail can be seen. For $w_{\rm AB}=1.55\sigma$, the attraction is sufficiently strong and long ranged that even our comparatively large simulation box is too small for $g(r)$ to reach its plateau. It should also be noted that due to the finite box size the bilayer composition far from the proteins does not necessarily approach $\frac{1}{2}$.

In the analytical theory outlined earlier the pair potential is described by Eq. (11b). It is determined by the variables a, ϕ_0^*, and λ, which, in turn, depend on the value of $w_{\rm AB}$; however, this dependence cannot be easily estimated. In Fig. 4 we attempt to approximately deduct the noncompositional component of the attraction by dividing out the pair correla-

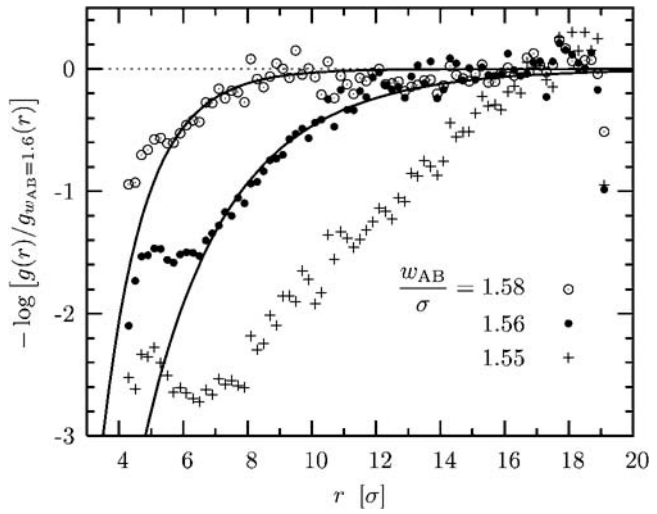

FIG. 4. Approximate pair potential due to composition effects, determined by subtracting the ideal-mixing contribution. The lines are large-distance fits to Eq. (11b).

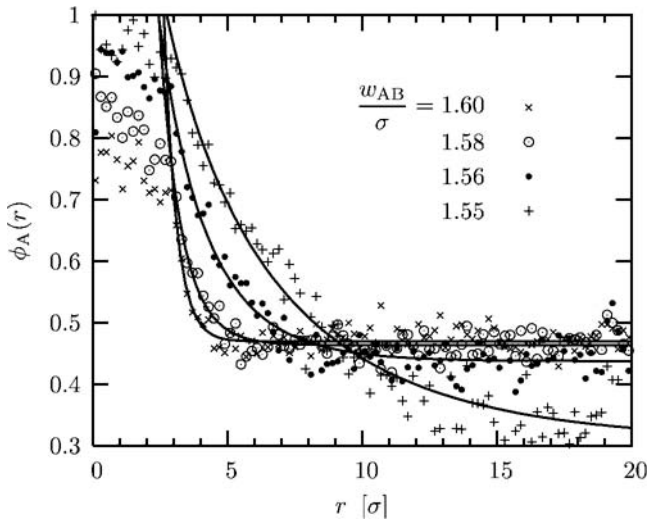

FIG. 5. Composition profile around adsorbed proteins for four different values of the incompatibility w_{AB}. The lines are three-parameter fits to the functional form $c_1+c_2K_0(r/\lambda)$, expected to hold if the decay follows the prediction of Eq. (8). The obtained values of λ are displayed in Table II.

tion function at ideal mixing (or, equivalently, subtracting the ideal-mixing potential). For $w_{AB}=1.58\sigma$ and 1.56σ the thus determined pair potentials level off within the separations realizable in our simulation box. Their large-distance behavior can be successfully fitted to Eq. (11b), yielding values of $\lambda=1.6\sigma$ and 3.4σ, respectively. As mentioned, for $w_{AB}=1.55\sigma$ the simulation box is too small to see the potential level off.

We also examine the concentration profile induced in the membrane by a single protein. Rather than performing additional simulations with a single protein we extract this information from the simulations of two proteins on a membrane discussed above. We select the simulation snapshots where the distance between the two proteins is greater than 15σ (20σ is the maximum for a box size of $40\sigma\times40\sigma$). In these snapshots we take two slices of the membrane of width 6σ perpendicular to the line connecting the two proteins and centered on each of them. Within these slices we measure the dependence of the composition of the membrane on the distance from the proteins. The results are displayed in Fig. 5.

For distances less than about 3σ, corresponding to the area directly below the adsorbed proteins, the composition is relatively constant. For $w_{AB}=1.6\sigma$ this plateau is roughly 0.75, whereas at $w_{AB}=1.55\sigma$ the fraction of A lipids is about 0.95. This difference is due to the fact that directly under the proteins the upper leaflet of the bilayer is pure lipid A, and the enrichment of A in the lower leaflet depends on the level of coupling. For $w_{AB}=1.60\sigma$ there is no coupling, thus the fraction of $0.75=\frac{1}{2}(1+\frac{1}{2})$, but at $w_{AB}=1.55\sigma$ there is almost complete coupling, hence the fraction of $0.95=\frac{1}{2}(1+0.9)$. Beyond the protein radius the volume fraction of A lipids drops and for $w_{AB}\geq1.56\sigma$ reaches a plateau level within the simulation box. The bulk concentration of A lipids decreases with decreasing w_{AB}. This is because as the area around the protein becomes enriched in lipid A, there is a concomitant depletion in the rest of the system.

The lines in the figure show three-parameter fits of the form $c_1+c_2K_0(r/\lambda)$. The values of the characteristic length λ obtained are shown in Table II, and their inverse are also plotted in Fig. 2, where they provide an independent means of localizing the critical point. The simple theory outlined in Sec. II D posits that this length is the same as the characteristic length occurring in the pair interaction. As Table II shows, this is not correct, though. In both cases for which parameters could be determined the pair interaction has a longer characteristic range than the single profile decay length. As mentioned above, upon approaching the critical point, composition fluctuations will additionally contribute in the form of a critical Casimir force and thereby renormalize the protein-protein interaction. Hence, the ground-state prediction of an identical one- and two-particle characteristic lengths should not be expected to hold.

C. Many proteins

Finally, we investigate protein aggregation by simulating large $80\sigma\times80\sigma$ membrane patches with 16 proteins adsorbed. Simulations were performed for values of w_{AB} ranging from 1.60σ to 1.56σ, although we only present snapshots here of the two extreme cases. The time scales for aggregation are extremely long and our system sizes are still rela-

TABLE II. Value of the characteristic length λ obtained from fitting the appropriate modified Bessel function to the data in Fig. 4 (pair potential) and Fig. 5 (single profile decay).

w_{AB}/σ	λ/σ (profile)	Fitting range	λ/σ (interaction)	Fitting range
1.60	0.5	3.0–10	⋯	⋯
1.58	0.9	3.0–20	1.6	5.5–10
1.56	2.4	3.0–20	3.4	6.5–12
1.55	6.6	3.0–20	⋯	⋯

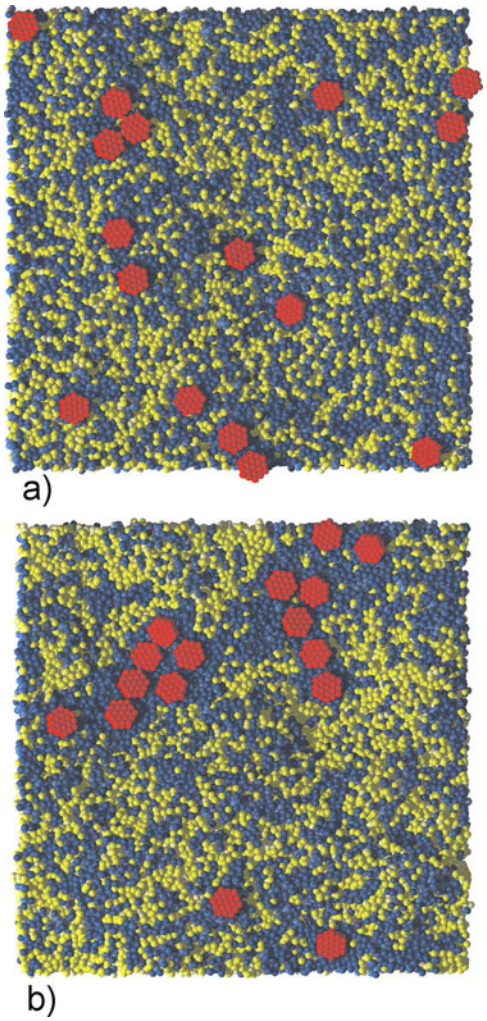

FIG. 6. (Color online) Top-view snapshots of mixed membranes onto which 16 proteins have adsorbed, after an equilibration time of $140\,000\tau$. (a) $w_{AB}=1.60\sigma$ (ideal lipid mixing); (b) $w_{AB}=1.56\sigma$ (strong compositional contribution to demixing and protein aggregation).

tively small, so it is not possible to ascertain whether macroscopic phase separation occurs. However, trends can be identified. In Fig. 6 we show two membrane snapshots taken after simulation times of $140\,000\tau$. Figure 6(a) shows a snapshot for $w_{AB}=1.60\sigma$ that shows a small degree of protein clustering consistent with the small minimum in the pair potential seen in Fig. 3. In contrast, Fig. 6(b), with $w_{AB}=1.56\sigma$, provides evidence for a significantly stronger aggregation behavior, and with sufficient time—and simulation size—one would presumably observe macroscopic phase separation.

Demixing as the ultimate consequence of composition-mediated protein interactions is intuitively reasonable: More energy is gained during protein adsorption to the preferred component if the other component is expelled from the binding region. This will also lower the *free* energy if the penalty associated with component demixing is small enough. The latter will always be the case sufficiently close to the critical point. Hence, one may conclude that the addition of a third preferentially solvating component increases the phase transition temperature. This is correct and can be proved on purely thermodynamic grounds.[88] While impressive by virtue of its generality, like every thermodynamic argument, quantifying the underlying microscopic physics nevertheless provides additional insight. For instance, it yields experimentally testable predictions for nonideal protein distributions which manifest *before* the system fully segregates, i.e., in the situation actually presumed to be relevant in biology.

V. SUMMARY AND CONCLUSIONS

In this work we studied the effect of a near-critical binary lipid mixture on selectively adsorbing proteins using coarse-grained molecular dynamics simulations. We analyzed our findings using a phenomenological Ginzburg-Landau theory, which can also be readily extended to curved geometries. The structure of the halos formed around proteins by the preferred lipid component compares well to the ground-state prediction of the theory. Halo overlap leads to lipid composition-mediated protein interactions, which are attractive in the symmetric case studied here and grow upon approaching the critical point. The resulting pair interaction, as measured in our simulations, compares qualitatively with the analytical prediction, after subtracting an additional noncompositional component of the force. However, in contrast to the simple ground-state calculation, the observed interaction range is longer than the decay length of one-particle halos, which points to the importance of critical composition fluctuations that also contribute to the attraction. Simulations of large membrane patches with 16 adsorbed proteins show a composition-driven formation of larger protein clusters. Selectively binding proteins thereby decrease the miscibility of lipids, as expected on thermodynamic grounds.

The models we used are evidently strongly simplified and cannot approach the full complexity of a real biological membrane. Yet, they illustrate that the expected physical principles of membrane mediated interactions by composition fields (or, in a previous work, curvature fields[46]), can be properly represented in particle-based off-lattice lipid bilayer models despite the large length and time scales involved. This opens exciting possibilities to systematically and in a statistically significant way treat combinations of these effects. One may thereby approach more closely situations which are believed to hold for actual biomembrane-protein systems and for which simple analytical results are much less readily available.

ACKNOWLEDGMENTS

The authors would like to thank Martin Müller, Jemal Guven, Burkhard Dünweg, Andreas Janshoff, and Sarah Veatch for stimulating discussions, and an anonymous referee for alerting us to Ref. 88. Financial support from SFB 625 (B.J.R.) and the German Science Foundation (Grant No. De775/1-3, MD) was also gratefully acknowledged.

[1] S. J. Singer and G. L. Nicolson, Science **175**, 720 (1972).
[2] D. A. Brown and E. London, Biochem. Biophys. Res. Commun. **240**, 1 (1997).

[3]K. Simons and E. Ikonen, Nature (London) **387**, 569 (1997).
[4]D. A. Brown and E. London, J. Membr. Biol. **164**, 103 (1998).
[5]D. A. Brown and E. London, Annu. Rev. Cell Dev. Biol. **14**, 111 (1998).
[6]D. A. Brown and E. London, J. Biol. Chem. **275**, 17221 (2000).
[7]S. L. Veatch and S. L. Keller, Phys. Rev. Lett. **89**, 268101 (2002).
[8]S. L. Veatch and S. L. Keller, Biophys. J. **85**, 3074 (2003).
[9]T. Baumgart, S. T. Hess, and W. W. Webb, Nature (London) **425**, 821 (2003).
[10]S. L. Veatch, I. V. Polozov, K. Gawrisch, and S. L. Keller, Biophys. J. **86**, 2910 (2004).
[11]S. L. Veatch and S. L. Keller, Phys. Rev. Lett. **94**, 148101 (2005).
[12]G. W. Feigenson, Annu. Rev. Biophys. Biomol. Struct. **36**, 63 (2007).
[13]T. Baumgart, A. T. Hammond, P. Sengupta, S. T. Hess, D. A. Holowka, B. A. Baird, and W. W. Webb, Proc. Natl. Acad. Sci. U.S.A. **104**, 3165 (2007).
[14]J. Fan, M. Sammalkorpi, and M. Haataja, Phys. Rev. Lett. **100**, 178102 (2008).
[15]J. Gomez, F. Sagues, and R. Reigada, Phys. Rev. E **77**, 021907 (2008).
[16]A. Kusumi *et al.*, Annu. Rev. Biophys. Biomol. Struct. **34**, 351 (2005).
[17]O. G. Mouritsen and M. Bloom, Biophys. J. **46**, 141 (1984).
[18]D. R. Fattal and A. Ben Shaul, Biophys. J. **65**, 1795 (1993).
[19]H. Aranda-Espinoza, A. Berman, N. Dan, P. Pincus, and S. Safran, Biophys. J. **71**, 648 (1996).
[20]C. Nielsen, M. Goulian, and O. S. Andersen, Biophys. J. **74**, 1966 (1998).
[21]S. May and A. Ben Shaul, Biophys. J. **76**, 751 (1999).
[22]S. May and A. Ben Shaul, Phys. Chem. Chem. Phys. **2**, 4494 (2000).
[23]T. Gil and J. H. Ipsen, Phys. Rev. E **55**, 1713 (1997).
[24]T. Gil, M. C. Sabra, J. H. Ipsen, and O. G. Mouritsen, Biophys. J. **73**, 1728 (1997).
[25]T. Gil, J. H. Ipsen, and C. F. Tejero, Phys. Rev. E **57**, 3123 (1998).
[26]T. Gil, J. H. Ipsen, O. G. Mouritsen, M. C. Sabra, M. M. Sperotto, and M. J. Zuckermann, Biochim. Biophys. Acta **1376**, 245 (1998).
[27]S. May, D. Harries, and A. Ben Shaul, Biophys. J. **79**, 1747 (2000).
[28]S. May, D. Harries, and A. Ben Shaul, Phys. Rev. Lett. **89**, 268102 (2002).
[29]E. C. Mbamala, A. Ben-Shaul, and S. May, Biophys. J. **88**, 1702 (2004).
[30]M. Goulian, R. Bruinsma, and P. Pincus, Europhys. Lett. **22**, 145 (1993).
[31]M. Goulian, R. Bruinsma, and P. Pincus, Europhys. Lett. **23**, 155 (1993).
[32]J.-M. Park and T. C. Lubensky, J. Phys. I France **6**, 1217 (1996).
[33]J. B. Fournier and P. G. Dommersnes, Europhys. Lett. **39**, 681 (1997).
[34]T. Weikl, M. Kozlov, and W. Helfrich, Phys. Rev. E **57**, 6988 (1998).
[35]P. G. Dommersnes, J. B. Fournier, and P. Galatola, Europhys. Lett. **42**, 233 (1998).
[36]P. Dommersnes and J.-B. Fournier, Eur. Phys. J. B **12**, 9 (1999).
[37]M. S. Turner and P. Sens, Biophys. J. **76**, 564 (1999).
[38]V. Marchenko and C. Misbah, Eur. Phys. J. E **8**, 477 (2002).
[39]J.-B. Fournier, P. Dommersnes, and P. Galatola, C. R. Biologies **326**, 467 (2003).
[40]D. Bartolo and J. Fournier, Eur. Phys. J. E **11**, 141 (2003).
[41]A. Evans, M. Turner, and P. Sens, Phys. Rev. E **67**, 041907 (2003).
[42]T. Weikl, Eur. Phys. J. E **12**, 265 (2003).
[43]P. Sens and M. Turner, Biophys. J. **86**, 2049 (2004).
[44]M. M. Müller, M. Deserno, and J. Guven, Europhys. Lett. **69**, 482 (2005).
[45]M. Müller, M. Deserno, and J. Guven, Phys. Rev. E **72**, 061407 (2005).
[46]B. Reynwar, G. Illya, V. Harmandaris, M. Mller, K. Kremer, and M. Deserno, Nature (London) **447**, 461 (2007).
[47]H. B. G. Casimir, Proc. K. Ned. Akad. Wet. **B51**, 793 (1948).
[48]M. E. Fisher, P. G. de Gennes, and C. R. Seances, C. R. Seances Acad. Sci., Ser. B **287**, 207 (1978).
[49]M. Krech, *The Casimir Effect in Critical Systems* (World Scientific, Singapore, 1994).
[50]M. Krech, Phys. Rev. E **56**, 1642 (1997).
[51]M. Krech, J. Phys.: Condens. Matter **11**, R391 (1999).
[52]C. Hertlein, L. Helden, A. Gambassi, S. Dietrich, and C. Bechinger, Nature (London) **451**, 172 (2008).
[53]R. R. Netz, Phys. Rev. Lett. **76**, 3646 (1996).
[54]F. Jähnig, Biophys. J. **36**, 329 (1981).
[55]R. Golestanian, M. Goulian, and M. Kardar, Europhys. Lett. **33**, 241 (1996).
[56]P. G. Dommersnes and J. B. Fournier, Europhys. Lett. **46**, 256 (1999).
[57]T. R. Weikl, Europhys. Lett. **54**, 547 (2001).
[58]W. Helfrich and T. R. Weikl, Eur. Phys. J. E **5**, 423 (2001).
[59]T. Taniguchi, Phys. Rev. Lett. **76**, 4444 (1996).
[60]P. B. S. Kumar and M. Rao, Phys. Rev. Lett. **80**, 2489 (1998).
[61]Y. Jiang, T. Lookman, and A. Saxena, Phys. Rev. E **61**, R57 (2000).
[62]J. L. McWhirter, G. Ayton, and G. A. Voth, Biophys. J. **87**, 3242 (2004).
[63]G. S. Ayton, J. L. McWhirter, P. McMurtry, and G. A. Voth, Biophys. J. **88**, 3855 (2005).
[64]Q. Shi and G. A. Voth, Biophys. J. **89**, 2385 (2005).
[65]A. Hanke, F. Schlesener, E. Eisenriegler, and S. Dietrich, Phys. Rev. Lett. **81**, 1885 (1998).
[66]F. Schlesener, A. Hanke, and S. Dietrich, J. Stat. Phys. **110**, 981 (2003).
[67]L. S. Brown, Ann. Phys. **126**, 135 (1980).
[68]E. Eisenriegler and M. Stapper, Phys. Rev. B **50**, 10009 (1994).
[69]J.-B. Fournier and C. Barbetta, Phys. Rev. Lett. **100**, 078103 (2008).
[70]S. A. Safran, *Statistical Thermodynamics of Surfaces, Interfaces, and Membranes* (Perseus, Cambridge, 1994).
[71]J. S. Rowlinson and B. Widom, *Molecular Theory of Capillarity* (Dover, Mineola, NY, 2002).
[72]J. J. Binney, N. J. Dowrick, A. J. Fisher, and M. E. J. Newman, *The Theory of Critical Phenomena* (Clarendon, Oxford, 1995).
[73]L. D. Landau and E. M. Lifshitz, *Theory of Elasticity* (Butterworth, Washington, DC/Heinemann, Oxford, 1999).
[74]R. Capovilla and J. Guven, J. Phys. A **35**, 6233 (2002).
[75]R. Capovilla and J. Guven, J. Phys.: Condens. Matter **16**, S2187 (2004).
[76]J. Guven, J. Phys. A **37**, L313 (2004).
[77]M. Do Carmo, *Differential Geometry of Curves and Surfaces* (Prentice Hall, Englewood Cliffs, NJ, 1976).
[78]E. Kreyszig, *Differential Geometry* (Dover, New York, 1991).
[79]M. Abramowitz and I. A. Stegun, *Handbook of Mathematical Functions* (Dover, New York, 1972).
[80]M. M. Nicolson, Proc. Cambridge Philos. Soc. **45**, 288 (1949).
[81]H.-J. Limbach, A. Arnold, B. A. Mann, and C. Holm, Comput. Phys. Commun. **174**, 704 (2006).
[82]I. Cooke, K. Kremer, and M. Deserno, Phys. Rev. E **72**, 011506 (2005).
[83]M. Müller, K. Katsov, and M. Schick, Phys. Rep. **434**, 113 (2006).
[84]M. Venturoli, M. M. Sperotto, M. Kranenburg, and B. Smit, Phys. Rep. **437**, 1 (2006).
[85]G. Brannigan, L. C. L. Lin, and F. L. H. Brown, Eur. Biophys. J. **35**, 104 (2006).
[86]A. Kolb and B. Dünweg, J. Chem. Phys. **111**, 4453 (1999).
[87]I. Cooke and M. Deserno, J. Chem. Phys. **123**, 224710 (2005).
[88]I. Prigogine and R. Defay, *Chemical Thermodynamics* (Longmans, Green, London, 1954).